Supporting Information

The accuracy challenge of DFT-based molecular assignment of ^{13}C MAS NMR characterization of surface intermediates in zeolite catalysis.

Alexander A. Kolganov[1], Anton A. Gabrienko[1,2], Ivan Yu. Chernyshov [3], Alexander G. Stepanov[1,2], Evgeny A. Pidko*[3,4]

[1]Boreskov Institute of Catalysis, Siberian Branch of the Russian Academy of Sciences,Prospekt Akademika Lavrentieva 5, Novosibirsk 630090, Russia

[2]Faculty of Natural Sciences, Department of Physical Chemistry, Novosibirsk State University, Pirogova Str. 2, Novosibirsk 630090, Russia

[3]TheoMAT Group, ChemBio Cluster, ITMO University, Lomonosova Street 9, Saint Petersburg, 191002, Russia

[4]Inorganic Systems Engineering group, Department of Chemical Engineering, Faculty of Applied Sciences, Delft University of Technology, Van der Maasweg 9, Delft 2629 HZ, The Netherlands

Section S1. Computational details for the periodic NMR chemical shifts calculatios .

The VASP program was used to calculate ^{13}C nuclear magnetic shielding tensors employing the gauge including projector augmented wave (GIPAW) algorithm [1]. Perdew, Burke, and Ernzerhof (PBE) [2] functionals with D3BJ dispersion correction[3,4] were adopted with the generalized gradient approximation (GGA) for the exchange correlation energy A plane-wave basis set with a cutoff energy of 600 eV in combination with the projected augmented wave (PAW) method was used. Brillouin zone-sampling was restricted to the Γ point. Linear responce method as implemented in VASP [1, 5] was used to obtain chemical shift values.

1. C. J. Pickard and F. Mauri, *Physical Review B*, 2001, **63**, 245101.
2. J. P. Perdew, K. Burke and Y. Wang, *Physical Review B*, 1996, **54**, 16533-16539.
3. S. Grimme, J. Antony, S. Ehrlich and H. Krieg, *Journal of Chemical Physics*, 2010, **132**.
4. S. Grimme, S. Ehrlich and L. Goerigk, *Journal of Computational Chemistry*, 2011, **32**, 1456-1465.
5. J. R. Yates, C. J. Pickard and F. Mauri, *Physical Review B*, 2007, **76**, 024401.

Table S1. σ_{ref} values for the different calculation protocols.

PBE-D3/aug-cc-pVDZ	Single point	191.3 ppm
	Optimized	190.8 ppm
PBE0-D3/aug-cc-pVDZ	Single point	195.1 ppm
	Optimized	196.4 ppm
wB97xD/aug-cc-pVDZ	Single point	195.5 ppm
	Optimized	196.8 ppm
HSE06/aug-cc-pVDZ	Single point	194.6 ppm
	Optimized	195.8 ppm
mPW1PW91/aug-cc-pVDZ	Single point	194.6 ppm
	Optimized	195.8 ppm
B3PW91-D3/aug-cc-pVDZ	Single point	193.7 ppm
	Optimized	195.0 ppm

Table S2. Periodic PBE energy of the various Si–O(CH_3)–Al methoxides.

Methoxide	Energy, kJ/mol	Methoxide	Energy, kJ/mol
T1–T2	17	T8–T9	17
T1–T5	20	T9–T6	0

T7–T7	83	T9–T9	24
T7–T8	10	T9–T10	3
T7–T11	16	T11–T12	5
T8–T7	1	T12–T12	27

Table S3. Calculated values of the ^{13}C NMR chemical shifts of the methoxides placed in the different position throughout zeolite framework.

Methoxide	PBE-D3/aug-cc-pVDZ (Single point)		PBE-D3/aug-cc-pVDZ (Optimized)	
	σ, ppm	δ	σ, ppm	δ
T1–T2	127.9	63.4	129.1	61.7
T1–T5	129.4	61.9	128.8	62.0
T7–T7	120.9	70.4	123.0	67.8
T7–T8	129.3	62.0	128.4	62.4
T7–T11	128.9	62.4	129.7	61.1
T8–T7	129.4	61.9	129.6	61.2
T8–T9	130.0	61.3	128.7	62.1
T9–T6	130.0	61.3	129.1	61.7
T9–T9	128.1	63.2	129.8	61.0
T9–T10	129.3	62.0	129.2	61.6
T11–T12	130.2	61.1	130.2	60.6
T12–T12	128.8	62.5	123.5	67.3
Methoxide	PBE0-D3/aug-cc-pVDZ (Single point)		PBE0-D3/aug-cc-pVDZ (Optimized)	
	σ, ppm	δ	σ, ppm	δ
T1–T2	132.4	62.7	137.0	59.3
T1–T5	133.9	61.2	136.6	59.8
T7–T7	125.8	69.3	132.3	64.0
T7–T8	133.8	61.3	136.7	59.7
T7–T11	133.3	61.8	137.9	58.5
T8–T7	133.8	61.3	137.7	58.7
T8–T9	134.3	60.9	137.1	59.3

T9–T6	134.4	60.7	137.1	59.3
T9–T9	132.6	62.5	137.5	58.8
T9–T10	133.9	61.3	137.7	58.7
T11–T12	134.5	60.6	137.8	58.6
T12–T12	133.3	61.8	137.7	58.6
Methoxide	wB97xD/aug-cc-pVDZ (Single point)		wB97xD /aug-cc-pVDZ (Optimized)	
	σ, ppm	δ	σ, ppm	δ
T1–T2	132.8	62.7	136.9	59.9
T1–T5	133.6	61.9	136.2	60.6
T7–T7	126.1	69.4	131.6	65.2
T7–T8	133.9	61.6	136.2	60.6
T7–T11	133.2	62.4	137.1	59.7
T8–T7	133.9	61.6	137.1	59.7
T8–T9	133.9	61.6	136.9	59.9
T9–T6	134.5	61.0	136.9	59.9
T9–T9	132.5	63.0	137.0	59.8
T9–T10	133.9	61.6	137.2	59.7
T11–T12	134.7	60.9	137.4	59.5
T12–T12	133.5	62.0	134.4	62.4
Methoxide	HSE06/aug-cc-pVDZ (Single point)		HSE06 /aug-cc-pVDZ (Optimized)	
	σ, ppm	δ	σ, ppm	δ
T1–T2	131.7	62.9	136.5	59.3
T1–T5	133.3	61.3	135.7	60.1
T7–T7	125.0	69.6	131.5	64.3
T7–T8	133.2	61.4	135.9	59.9
T7–T11	132.7	61.9	137.3	58.5
T8–T7	133.2	61.4	136.9	59.0
T8–T9	133.6	61.0	136.6	59.2
T9–T6	133.9	60.7	136.1	59.7
T9–T9	132.0	62.6	135.6	60.2

T9–T10	133.2	61.4	136.8	59.0
T11–T12	133.8	60.8	137.0	58.8
T12–T12	132.6	62.0	136.8	59.1
Methoxide	mPW1PW91/aug-cc-pVDZ (Single point)		mPW1PW91 /aug-cc-pVDZ (Optimized)	
	σ, ppm	δ	σ, ppm	δ
T1–T2	131.8	62.8	136.8	59.1
T1–T5	133.3	61.3	135.9	59.9
T7–T7	125.4	69.3	132.2	63.6
T7–T8	133.3	61.3	136.3	59.5
T7–T11	132.8	61.8	137.8	58.1
T8–T7	133.2	61.4	137.2	58.7
T8–T9	133.7	61.0	137.0	58.8
T9–T6	133.8	60.8	136.3	59.5
T9–T9	132.1	62.6	135.4	60.4
T9–T10	133.3	61.3	137.2	58.6
T11–T12	133.9	60.7	137.4	58.5
T12–T12	132.8	61.9	137.1	58.7
Methoxide	B3PW91-D3/aug-cc-pVDZ (Single point)		B3PW91-D3 /aug-cc-pVDZ (Optimized)	
	σ, ppm	δ	σ, ppm	δ
T1–T2	130.7	63.0	134.8	60.2
T1–T5	132.1	61.6	134.4	60.6
T7–T7	124.2	69.5	129.8	65.2
T7–T8	132.2	61.5	134.4	60.6
T7–T11	131.7	62.0	135.6	59.4
T8–T7	132.1	61.6	135.4	59.6
T8–T9	132.5	61.2	134.4	60.6
T9–T6	132.6	61.1	134.9	60.0
T9–T9	130.9	62.8	135.8	59.2
T9–T10	132.2	61.5	135.3	59.6
T11–T12	132.8	60.9	135.4	59.6

T12–T12	132.8	60.9	132.2	62.8

Table S4. Mean calculated ^{13}C chemical shifts and their value deviations.

Single point calculations				Cluster geometry optimization			
Methoxide	Mean ^{13}C chem. shift, ppm	Methoxide	Mean ^{13}C chem. shift, ppm	Methoxide	Mean ^{13}C chem. shift, ppm	Methoxide	Mean ^{13}C chem. shift, ppm
T1–T2	62.9 ± 0.3	T8–T9	61.0 ± 0.2	T1–T2	59.9 ± 1.0	T8–T9	59.9 ± 1.2
T1–T5	61.5 ± 0.3	T9–T6	60.9 ± 0.2	T1–T5	60.5 ± 0.8	T9–T6	60.0 ± 0.9
T7–T7	69.6 ± 0.4	T9–T9	62.8 ± 0.3	T7–T7	65.0 ± 1.5	T9–T9	59.9 ± 0.8
T7–T8	61.5 ± 0.3	T9–T10	61.5 ± 0.3	T7–T8	60.4 ± 1.0	T9–T10	59.5 ± 1.1
T7–T11	62.1 ± 0.3	T11–T12	60.8 ± 0.2	T7–T11	59.2 ± 1.0	T11–T12	59.3 ± 0.8
T8–T7	61.5 ± 0.2	T12–T12	61.8 ± 0.5	T8–T7	59.5 ± 1.1	T12–T12	61.2 ± 3.4

Table S5. Calculated values of the ^{13}C NMR chemical shifts of the various possible methane activation products adsorbed on the MFI zeolite framework.

Methoxide	PBE-D3/aug-cc-pVDZ (Single point)		PBE-D3/aug-cc-pVDZ (Optimized)	
	σ, ppm	δ, ppm	σ, ppm	δ, ppm
$Si(OCH_3)Al$	127.9	63.4	129.1	61.7
$CH_3OH..BAS$	138.3	52.5	143.9	48.6
$(CH_3)_2O$ – atom 1	121.0	69.8	129.2	63.3
$(CH_3)_2O$ – atom 2	124.7	66.1	129.2	63.3
$(CH_3)_2O$ – mean	122.8	68.0	129.2	63.3
$Cu..CH_3OH$	125.5	65.3	129.1	63.4
Cu.. $(CH_3)_2O$ – atom 1	117.7	73.1	119.2	73.3
Cu.. $(CH_3)_2O$ – atom 2	116.6	74.2	120.9	71.6
Cu.. $(CH_3)_2O$ – mean	117.2	73.6	120.0	72.5
$[Cu(\mu\text{-}OCH_3)Cu]^{2+}$	121.5	69.3	122.6	69.9
$[Cu(\mu\text{-}CH_3OH)Cu]^{2+}$	109.8	81.0	114.1	78.4

$Si(OCH_3)Al$ .. $[Cu(\mu\text{-}OH)Cu]^+$	127.6	63.2	126.9	65.6
Methoxide	PBE0-D3/aug-cc-pVDZ (Single point)		PBE0-D3/aug-cc-pVDZ (Optimized)	
	σ, ppm	δ, ppm	σ, ppm	δ, ppm
$Si(OCH_3)Al$	132.4	62.7	137.0	59.3
CH_3OH..BAS	143.0	52.1	146.8	49.6
$(CH_3)_2O$ – atom 1	126.7	68.4	137.5	58.8
$(CH_3)_2O$ – atom 2	130.3	64.8	134.9	61.4
$(CH_3)_2O$ – mean	128.5	66.6	136.2	60.1
Cu..CH_3OH	131.6	63.5	138.2	58.2
Cu.. $(CH_3)_2O$ – atom 1	124.2	70.9	129.3	67.1
Cu.. $(CH_3)_2O$ – atom 2	123.2	71.9	129.6	66.7
Cu.. $(CH_3)_2O$ – mean	123.7	71.4	129.5	66.9
$[Cu(\mu\text{-}OCH_3)Cu]^{2+}$	128.6	66.5	132.2	64.1
$[Cu(\mu\text{-}CH_3OH)Cu]^{2+}$	118.1	77.0	126.3	70.1
$Si(OCH_3)Al$ .. $[Cu(\mu\text{-}OH)Cu]^+$	131.8	63.3	137.3	59.0
Methoxide	wB97xD/aug-cc-pVDZ (Single point)		wB97xD /aug-cc-pVDZ (Optimized)	
	σ, ppm	δ, ppm	σ, ppm	δ, ppm
$Si(OCH_3)Al$	132.8	62.7	136.9	59.9
CH_3OH..BAS	143.1	52.4	146.6	50.3
$(CH_3)_2O$ – atom 1	127.2	68.3	138.0	58.8
$(CH_3)_2O$ – atom 2	130.7	64.8	135.7	61.1
$(CH_3)_2O$ – mean	129.0	66.5	136.9	60.0
Cu..CH_3OH	131.7	63.8	138.2	58.7
Cu.. $(CH_3)_2O$ – atom 1	125.0	70.6	128.9	67.9
Cu.. $(CH_3)_2O$ – atom 2	123.6	71.9	129.7	67.2
Cu.. $(CH_3)_2O$ – mean	124.3	71.2	129.3	67.5
$[Cu(\mu\text{-}OCH_3)Cu]^{2+}$	129.3	66.2	132.3	64.5

$[Cu(\mu\text{-}CH_3OH)Cu]^{2+}$	118.2	77.3	126.5	70.3
$Si(OCH_3)Al$ .. $[Cu(\mu\text{-}OH)Cu]^{+}$	130.7	64.8	137.7	59.1
Methoxide	HSE06/aug-cc-pVDZ (Single point)		HSE06 /aug-cc-pVDZ (Optimized)	
	σ, ppm	δ, ppm	σ, ppm	δ, ppm
$Si(OCH_3)Al$	131.7	62.9	136.5	59.3
CH_3OH..BAS	142.5	52.2	146.8	49.1
$(CH_3)_2O$ – atom 1	126.0	68.6	136.8	59.0
$(CH_3)_2O$ – atom 2	129.7	64.9	136.6	59.2
$(CH_3)_2O$ – mean	127.9	66.7	136.7	59.1
Cu..CH_3OH	131.0	63.6	137.1	58.8
Cu.. $(CH_3)_2O$ – atom 1	123.7	70.9	128.7	67.2
Cu.. $(CH_3)_2O$ – atom 2	122.5	72.1	129.6	66.3
Cu.. $(CH_3)_2O$ – mean	123.1	71.5	129.1	66.7
$[Cu(\mu\text{-}OCH_3)Cu]^{2+}$	127.9	66.7	131.5	64.3
$[Cu(\mu\text{-}CH_3OH)Cu]^{2+}$	117.5	77.1	125.0	70.8
$Si(OCH_3)Al$ .. $[Cu(\mu\text{-}OH)Cu]^{+}$	130.9	63.7	136.3	59.6
Methoxide	mPW1PW91/aug-cc-pVDZ (Single point)		mPW1PW91 /aug-cc-pVDZ (Optimized)	
	σ, ppm	δ, ppm	σ, ppm	δ, ppm
$Si(OCH_3)Al$ CH_3OH..BAS	131.8	62.8	136.8	59.1
$(CH_3)_2O$ – atom 2	142.5	52.2	147.0	48.8
$(CH_3)_2O$ – atom 1	126.5	68.1	137.6	58.3
$(CH_3)_2O$ – atom 2	130.0	64.6	137.1	58.7
$(CH_3)_2O$ – mean	128.3	66.4	137.4	58.5
Cu..CH_3OH	131.2	63.4	137.4	58.5
Cu.. $(CH_3)_2O$ – atom 1	123.8	70.8	130.0	65.8
Cu.. $(CH_3)_2O$ – atom	123.0	71.7	130.5	65.3

2				
Cu.. $(CH_3)_2O$ – mean	123.4	71.2	130.3	65.5
$[Cu(\mu\text{-}OCH_3)Cu]^{2+}$	128.5	66.1	132.6	63.3
$[Cu(\mu\text{-}CH_3OH)Cu]^{2+}$	117.9	76.7	125.8	70.0
$Si(OCH_3)Al$ .. $[Cu(\mu\text{-}OH)Cu]^{+}$	131.1	63.5	136.8	59.0
Methoxide	B3PW91-D3/aug-cc-pVDZ (Single point)		B3PW91-D3 /aug-cc-pVDZ (Optimized)	
	σ, ppm	δ, ppm	σ, ppm	δ, ppm
$Si(OCH_3)Al$	130.7	63.0	134.8	60.2
CH_3OH..BAS	141.4	52.4	144.9	50.1
$(CH_3)_2O$ – atom 1	125.3	68.4	136.2	58.7
$(CH_3)_2O$ – atom 2	128.8	64.9	134.1	60.9
$(CH_3)_2O$ – mean	127.0	66.7	135.2	59.8
Cu..CH_3OH	129.9	63.8	136.2	58.8
Cu.. $(CH_3)_2O$ – atom 1	122.5	71.3	126.4	68.5
Cu.. $(CH_3)_2O$ – atom 2	121.5	72.2	128.2	66.8
Cu.. $(CH_3)_2O$ – mean	122.0	71.7	127.3	67.7
$[Cu(\mu\text{-}OCH_3)Cu]^{2+}$	127.1	66.6	130.2	64.7
$[Cu(\mu\text{-}CH_3OH)Cu]^{2+}$	116.3	77.4	124.2	70.8
$Si(OCH_3)Al$ .. $[Cu(\mu\text{-}OH)Cu]^{+}$	130.0	63.7	135.0	60.0

Table S6. Mean calculated ^{13}C chemical shifts of the possible methane and their value deviations.

Single point calculations				Cluster geometry optimization			
Methoxide	Mean ^{13}C chem. shift, ppm	Methoxide	Mean ^{13}C chem. shift, ppm	Methoxide	Mean ^{13}C chem. shift, ppm	Methoxide	Mean ^{13}C chem. shift, ppm
$Si(OCH_3)Al$	62.9 ± 0.3	Cu.. $(CH_3)_2O$ – atom 1	71.3 ± 0.9	$Si(OCH_3)Al$	59.9 ± 1.0	Cu.. $(CH_3)_2O$ – atom 1	68.3 ± 2.6
CH_3OH..BAS	52.3 ± 0.2	Cu.. $(CH_3)_2O$ –	72.4 ± 0.9	CH_3OH..BAS	50.1 ± 1.5	Cu.. $(CH_3)_2O$ –	67.3 ± 2.2

		atom 2				atom 2	
$(CH_3)_2O$ – atom 1	68.6 ± 0.6	Cu.. $(CH_3)_2O$ – mean	70.2 ± 2.4	$(CH_3)_2O$ – atom 1	59.5 ± 1.9	Cu.. $(CH_3)_2O$ – mean	67.8 ± 2.4
$(CH_3)_2O$ – atom 2	65.0 ± 0.5	$[Cu(\mu\text{-}OCH_3)Cu]^{2+}$	67.0 ± 1.3	$(CH_3)_2O$ – atom 2	60.7 ± 1.7	$[Cu(\mu\text{-}OCH_3)Cu]^{2+}$	65.5 ± 2.3
$(CH_3)_2O$ – mean	66.8 ± 0.6	$[Cu(\mu\text{-}CH_3OH)Cu]^{2+}$	77.7 ± 1.6	$(CH_3)_2O$ – mean	60.1 ± 1.6	$[Cu(\mu\text{-}CH_3OH)Cu]^{2+}$	71.7 ± 3.3
$Cu..CH_3OH$	63.9 ± 0.7	$Si(OCH_3)Al$ .. $[Cu(\mu\text{-}OH)Cu]^{+}$	63.7 ± 0.6	$Cu..CH_3OH$	59.4 ± 1.9	$Si(OCH_3)Al$ .. $[Cu(\mu\text{-}OH)Cu]^{+}$	60.6 ± 2.8

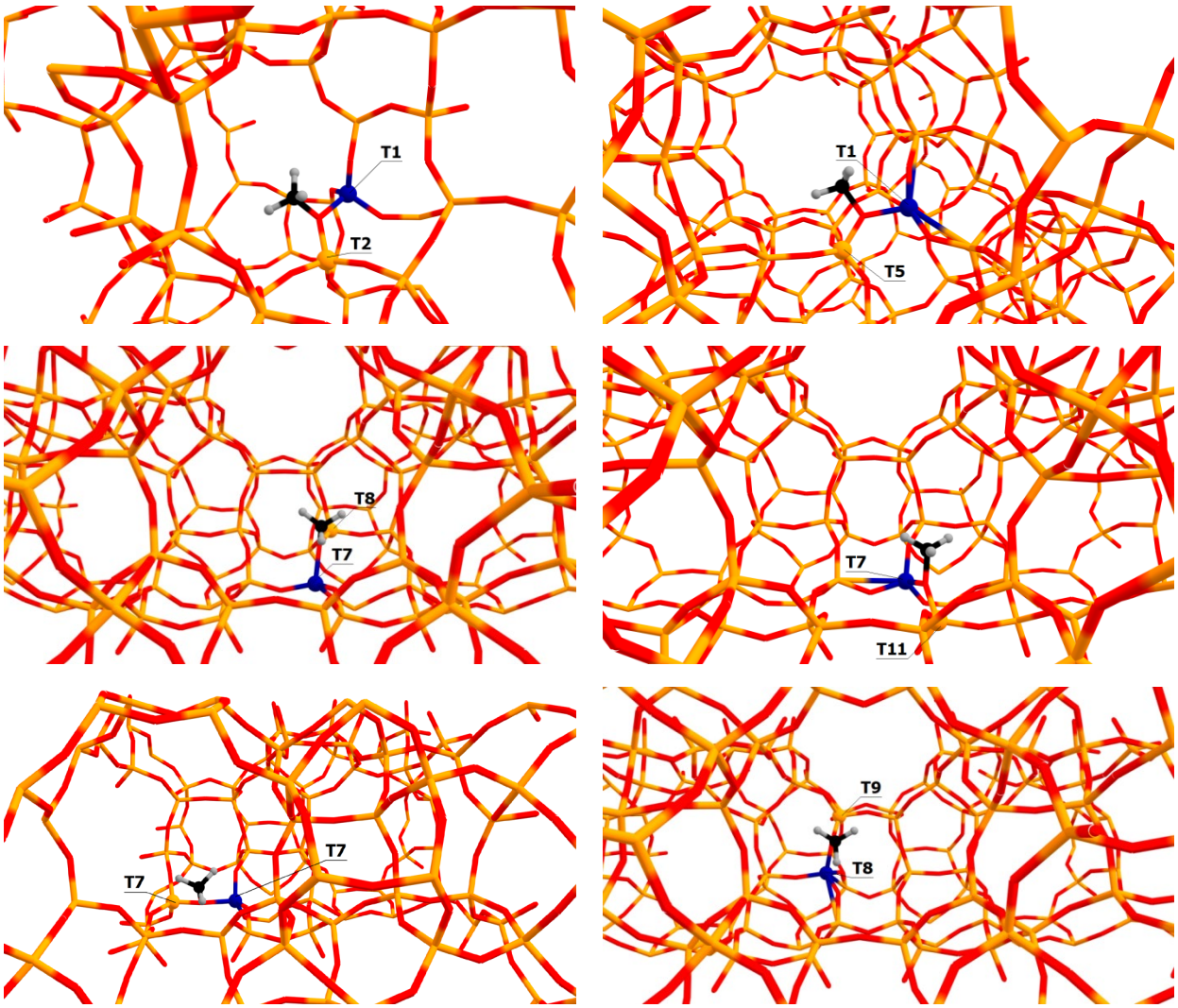

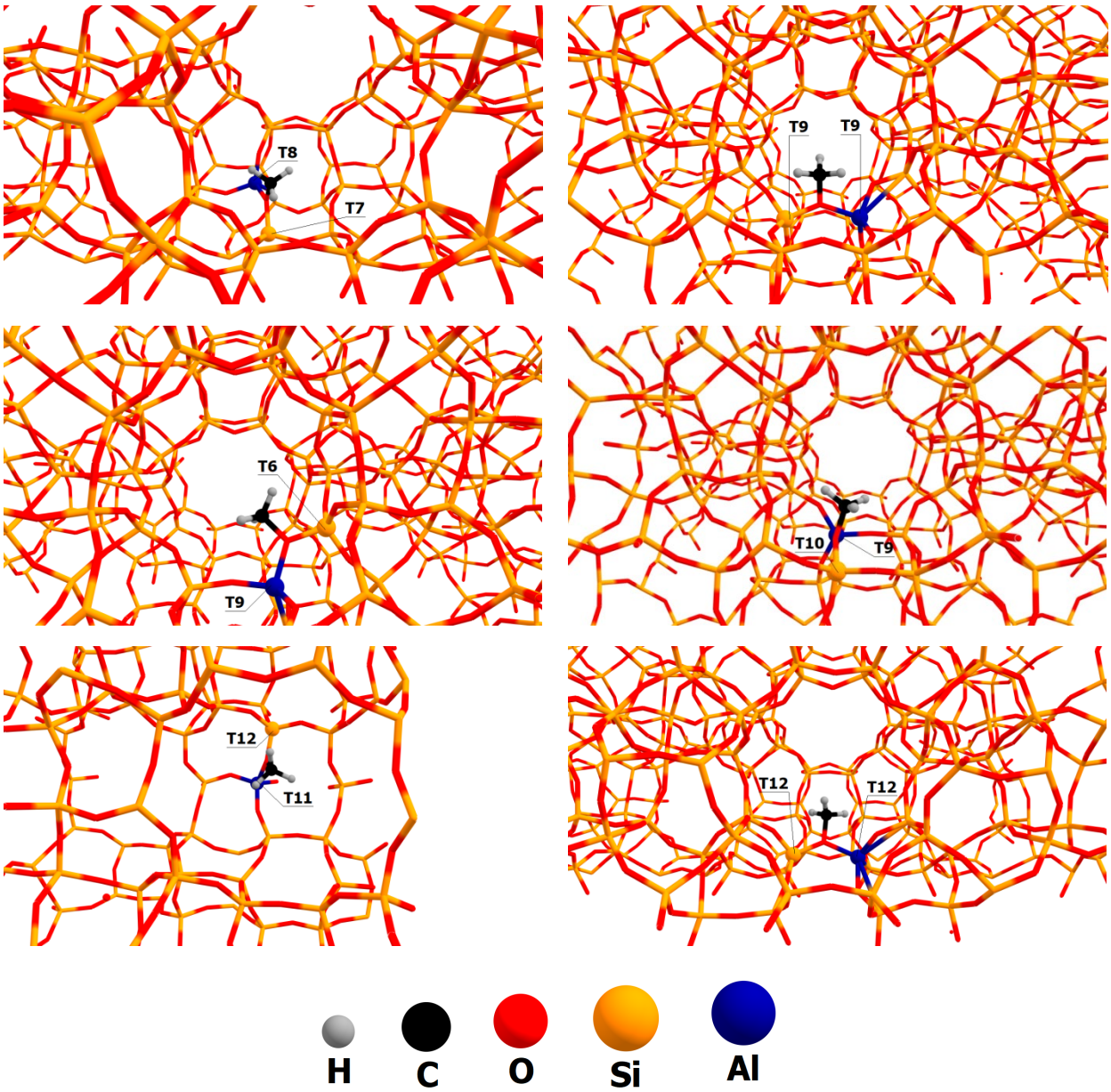

Figure S1. Optimized structures of the methoxides used for the calculations.

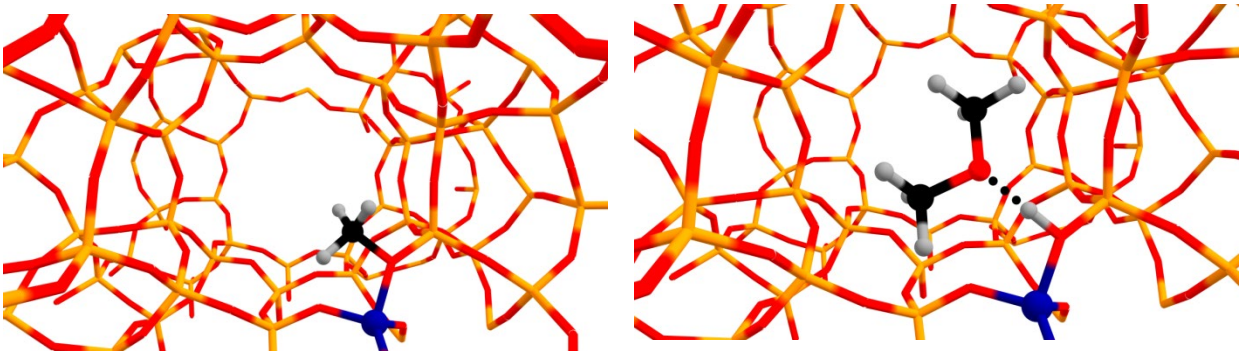

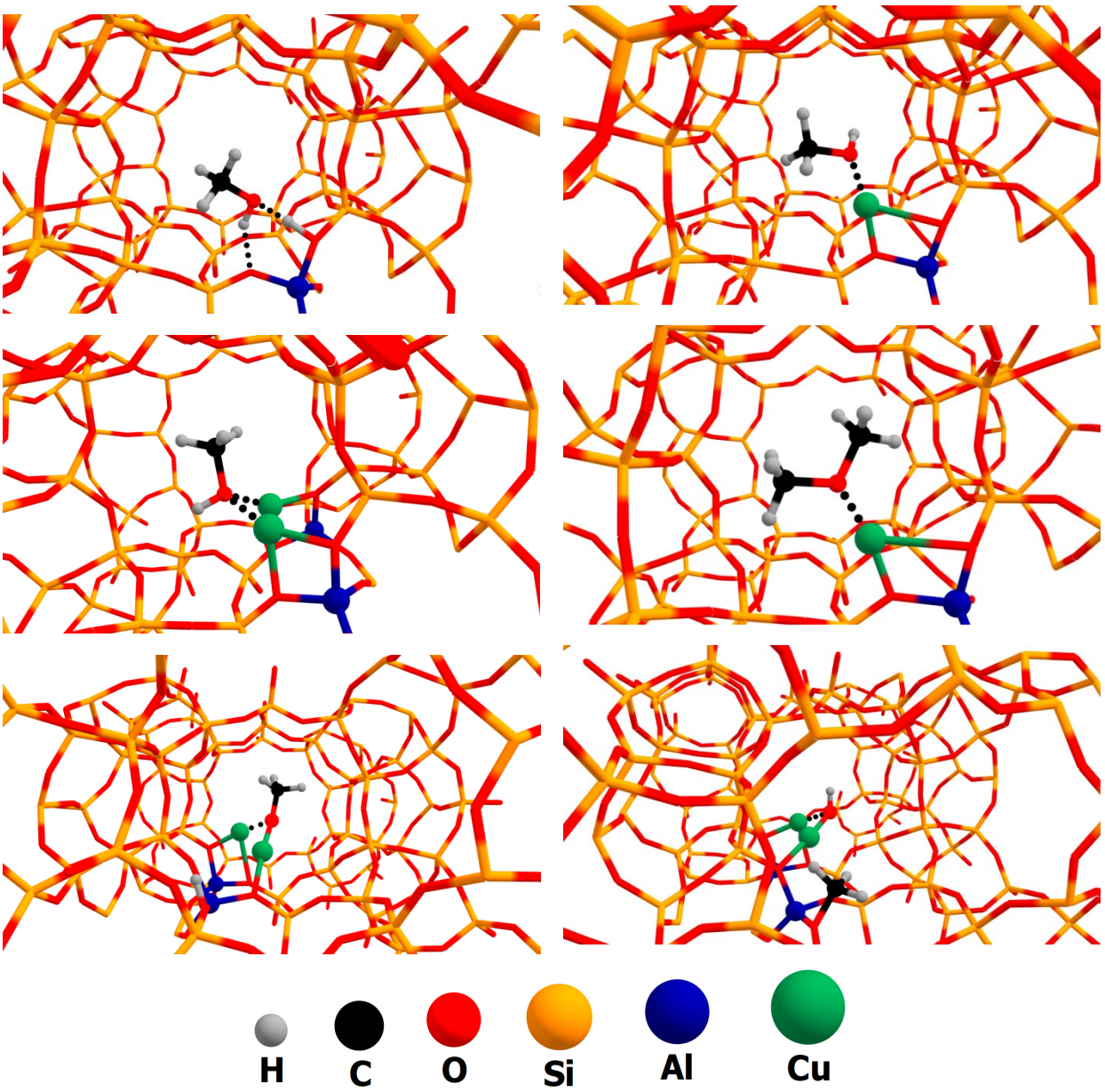

Figure S2. Optimized structure of the methane activation adsorbed products used for the ^{13}C NMR chemical shifts calculations. On left: $SiO(CH_3)Al$ methoxide, methanol adsorbed on Bronsted acid site, methanol adsorbed between two copper atoms $[Cu(\mu\text{-}CH_3OH)Cu]^{2+}$, methoxide $[Cu(\mu\text{-}OCH_3)Cu]^{2+}$. On the right: dimethyl ether adsorbed on BAS, methanol adsorbed on Cu^+ cation, dimethyl ether adsorbed on Cu^+ cation, and $Si(OCH_3)Al$ methoxide adsorbed near the $[Cu(\mu\text{-}OH)Cu]^+$ site.

Figure S3. Optimized structures of the intermediates containing $[Cu(\mu\text{-}O)Cu]^{2+}$ core and their energies.

Structure	Optimized geometry	Relative energy,(kJ/mol)

Methane adsorbed on $[Cu(\mu\text{-}O)Cu]^{2+}$ site	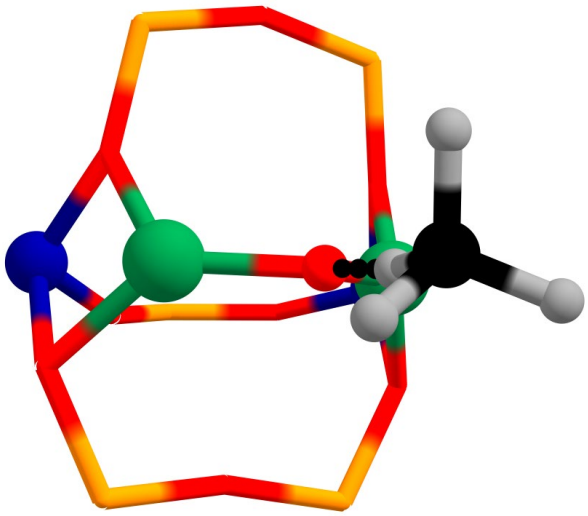	0
$[Cu(\mu\text{-}CH_3OH)Cu]^{2+}$	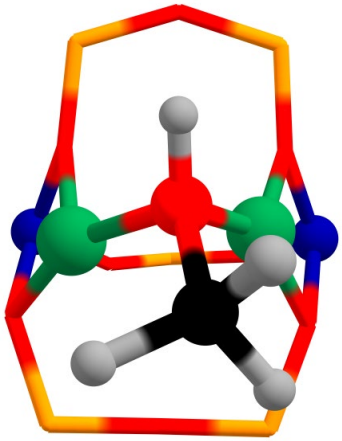	-148
$[Cu(\mu\text{-}OCH_3)Cu]^{2+}$	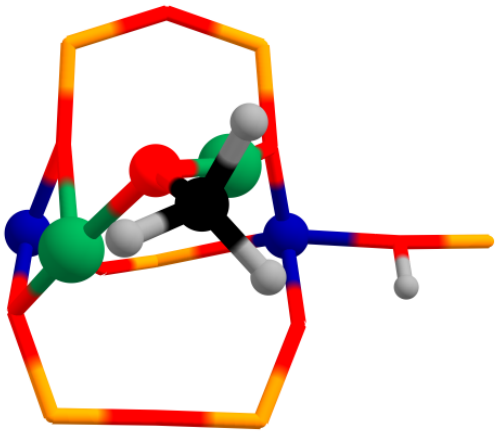	-105

$Si(OCH_3)Al$ methoxide near the $[Cu(\mu\text{-}OH)Cu]^+$ site	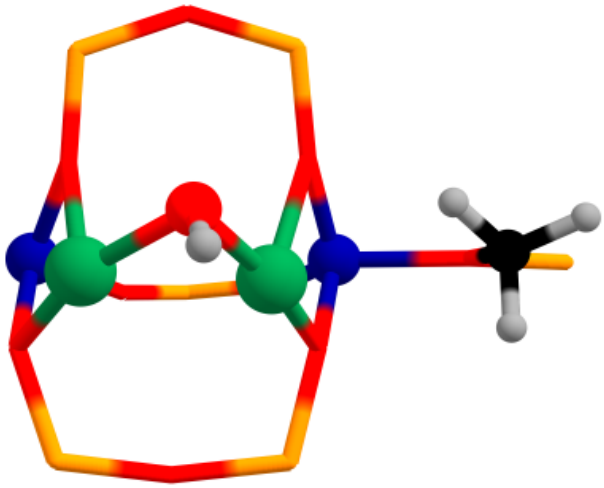	-73

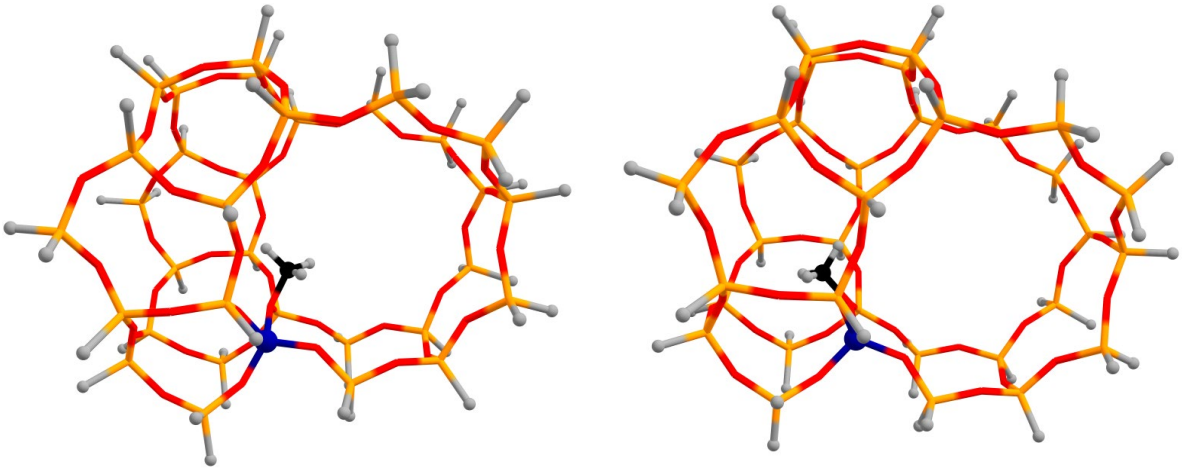

Figure S4. Cluster structure constructed from the optimized structure of T12–T12 methoxide (left) and optimized geometry of this cluster (right).

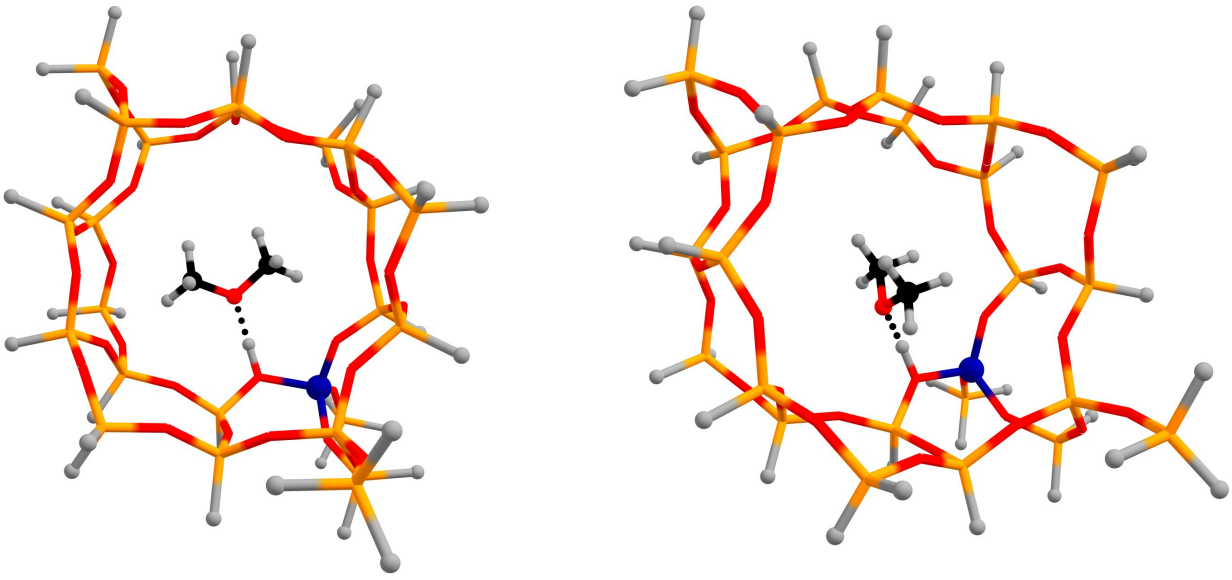

Figure S5. Cluster structure constructed from the optimized structure of dimethyl ether adsorbed on BAS (left) and optimized geometry of this cluster (right).

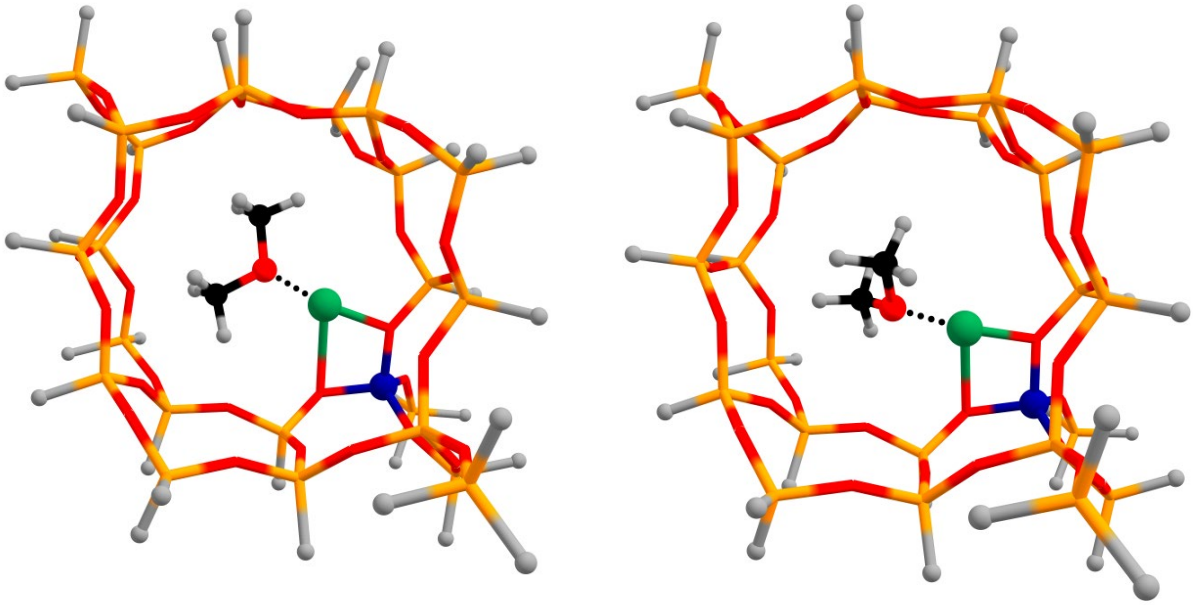

Figure S6. Cluster structure constructed from the optimized structure of dimethyl ether adsorbed on Cu^{+} cation (left) and optimized geometry of this cluster (right).